Ab initio studies of isomerization and dissociation reactions of methyl peroxynitrate

ARTICLE *in* STRUCTURAL CHEMISTRY · JUNE 2014

Impact Factor: 1.84 · DOI: 10.1007/s11224-013-0351-9

5 AUTHORS, INCLUDING:

Renhui Zheng
Chinese Academy of Sciences
55 PUBLICATIONS **445** CITATIONS

Struct Chem (2014) 25:859–871
DOI 10.1007/s11224-013-0351-9

ORIGINAL RESEARCH

Ab initio studies of isomerization and dissociation reactions of methyl peroxynitrate

Wen-mei Wei · Ren-hui Zheng · Yun-kai Wu · Yue-li Pan · Fan Yang

Received: 7 August 2013 / Accepted: 17 September 2013 / Published online: 29 September 2013

Abstract Using the CCSD(T)/cc-pVDZ//B3LYP/6-311G(2d,2p) method, we calculated the detailed potential energy surfaces (PESs) for the unimolecular isomerization and decomposition of methyl peroxynitrate ($CH_3O_2NO_2$). The results show that there are the two most stable isomers, IS1a and IS1b, which are a pair of mirror image isomers. From IS1a and IS1b, different isomerization and unimolecular decomposition reaction channels have been studied and discussed. Among them, the predominant thermal decomposition pathways are those leading to $CH_3O_2 + NO_2$ and *cis*-$CH_3ONO + O_2$. The former is the lowest-energy path through the direct O–N bond rupture in IS1a or IS1b. The PES along the O–N bond in IS1a has been scanned, where the energy of IS1a reaches maximum value of 23.5 kcal/mol when the O–N bond is stretched to about 2.8 Å. This energy is 2.7 kcal/mol larger than the O–N bond dissociation energy (BDE) and 2.8 kcal/mol larger than the experimental active energy. In addition, because the energy barriers of IS1a isomerization to IS2a are 23.8 kcal/mol, close to the 20.8 kcal/mol O–N BDE in IS1a or IS1b, the isomerization reaction may compete with the direct bond rupture dissociation reaction.

W. Wei (✉) · Y. Wu · Y. Pan · F. Yang
Department of Chemistry, College of Basic Medicine, Anhui Medical University, Hefei 230032, Anhui, People's Republic of China
e-mail: cherrywwm@ustc.edu

R. Zheng (✉)
Beijing National Laboratory for Molecular Sciences, State Key Laboratory for Structural Chemistry of Unstable and Stable Species, Institute of Chemistry, Chinese Academy of Sciences, Zhongguancun, Beijing 100190, People's Republic of China
e-mail: zrh@iccas.ac.cn

Keywords Methyl peroxynitrate · Ab initio · Isomerization · Dissociation · Potential energy surface

Introduction

Ozone in the upper troposphere is an efficient greenhouse gas (0.25–0.65 Wm^{-2}) [1] with a long chemical lifetime (100–365 days) [2, 3]. Peroxynitrates (RO_2NO_2) influence tropospheric ozone production and the abundance of OH in both the troposphere and stratosphere. Non-acyl peroxynitrates such as HO_2NO_2 and $CH_3O_2NO_2$ are increasingly important at temperatures below 240 K, because the molecules are very weakly bound and rapidly dissociate at higher temperature [4]. Consequently, these molecules are most important in the stratosphere and upper troposphere. However, knowledge of the chemistry of alkyl RO_2NO_2 species is limited because they are difficult to isolate in the laboratory or to observe directly in the atmosphere [4]. Using the flash photolysis/ultraviolet absorption technique, Sander and Watson have measured the rate constants for the reaction $CH_3O_2 + NO_2 + M \rightleftharpoons CH_3O_2NO_2 + M$ (1) at 298 K over the pressure range 50–70 torr [5]. Employing the technique of pulsed laser photolysis–long path laser absorption, Ravishankara et al. [6] have studied the kinetics of the reaction (1) in N_2 over the temperature range 253–353 K. Zabel et al. [7] have investigated the thermal decomposition reaction of methyl peroxynitrate ($CH_3O_2NO_2$) via O–N bond fission in N_2 in a wide temperatures and pressure range, and determined the limiting low- and high-pressure rate constants. Then they suggested that $CH_3O_2NO_2$ is an important reservoir for both NO_x and CH_3O_2 radicals in the upper troposphere and the lower stratosphere. Bridier et al. [8] have studied the equilibrium

reaction (1) directly over the temperature range 333–373 K at atmospheric pressure using the flash photolysis and gave a value of equilibrium constant as a function of temperature. And Golden has examined the data for the system reaction (1) and drawn to the summary that there is significant uncertainty in the theory of unimolecular reactions, particularly with respect to energy transfer, and there are difficulties in obtaining various physical parameters derived from the poorly described potential energy surfaces (PESs) that have been obtained [9]. Therefore, the present work investigates the detailed PESs of $CH_3O_2NO_2$ at CCSD(T)/cc-pVDZ//B3LYP/6-311G(2d,2p) level of theory, in an attempt to elucidate the mechanisms of the isomerization and decomposition of $CH_3O_2NO_2$ in gas phase. Based on the calculated results, the possible dissociation mechanism of $CH_3O_2NO_2$ is proposed.

Computational methods

In this work using Becke's three-parameter hybrid exchange functional and the LYP correlation functional (B3LYP) in conjunction with the split valence polarized basis set 6-311G(2d,2p), geometry optimization of the reactants (IS), transition states (TS), and products were performed [10, 11]. The characteristic of these structures and their zero-point vibrational energies (ZPE, scaled by a factor of 0.96 [12]) were determined from frequency calculations at the same level. The optimized structure on the PES can be characterized as a transition state if only one imaginary frequency exists, or as a minima if all non-zero frequencies are real. Intrinsic reaction coordinate (IRC [13]) calculations were traced to insure that the transition states did in fact connect the proper minima. To improve the accuracy of the calculated barrier heights, the coupled-cluster theory with single, double, and triple excitations (CCSD(T) method) [14] with Dunning's correlation-consistent double-ζ basis set (cc-pVDZ) [15] was used to calculate the final electronic energies at the B3LYP/6-311G(2d,2p) optimized geometries. Unless otherwise specified, the CCSD(T)/cc-pVDZ relative energies (in kcal/mol) are used in the following discussions, by taking the energy of IS1a (−394.38551 Hartree) as zero for reference. We have carried out additional calculations using the quadratic configuration interaction level of theory with single, double, and triple excitations QCISD(T) method [16] with 6-311G(d,p) basis set to confirm the energies obtained by the CCSD(T)/cc-pVDZ method. And the energies were also calculated using the methods of CCSD(T)/6-311G(d,p), CBS-QB3 [17, 18], G3B3, and G3MP2B3 [19, 20], respectively. The calculations show that the energies obtained at different levels of theories are in good agreement. All calculations are performed with the Gaussian 03 package [21].

Results and discussion

Ten isomers and eight pathways to produce different products have been studied for the isomerization and dissociation reactions of methyl peroxynitrate. The optimized geometries of stationary points are depicted in Fig. 1. The CCSD(T)/cc-pVDZ relative energies and zero-point vibrational energies of stationary points calculated at the B3LYP/6-311G(2d,2p) level are presented in Table 1, with the energies calculated using other methods. The schematic profiles of the CCSD(T)/cc-pVDZ PESs for the title reaction are plotted in Figs. 2 and 3.

Isomerizations of $CH_3O_2NO_2$

IS1, $CH_3O_2NO_2$

In the optimized geometries of stationary points of $CH_3O_2NO_2$ there are two stereoisomers, IS1a and IS1b, which are a pair of mirror image isomers. In the structures of IS1a, the length of C_1—O_2 bond is 1.430 Å, and it is 1.433 Å in IS1b. The O_2—O_6 bond in IS1b is 1.404 Å, only 0.001 Å longer than in IS1a. However, the O_6—N_7 bond in IS1b is 1.509 Å, 0.001 Å shorter than in IS1a. And the N_7—O_8 and N_7—O_9 bonds have the same lengths in IS1a and IS1b, respectively. Besides, this pair of enantiomers almost has the same bond angles among the same three atoms. The main difference between the structures of IS1a and IS1b is that the dihedral angle among C_1, O_2, O_6, and N_7 atoms is 94.7° in IS1a, while it is −94.8° in IS1b. From the calculated results, IS1a and IS1b have the same energies. Golden [9] has computed the structure and frequencies for $CH_3O_2NO_2$ at the B3LYP/6-311 + G** level using Spartan. Our calculated S_{tot} of IS1a and IS1b are both 78.1 cal mol^{-1} K^{-1}, which agrees well with Golden's 78.39 cal mol^{-1} K^{-1}. The frequencies that we calculated is about 2–10 cm^{-1} larger than Golden's, respectively, which are also in good agreement.

IS2, CH_3O_2ONO

There are four conformations of IS2, i.e., IS2a, IS2b, IS2c, and IS2d. The energies of them are about 24.7, 22.5, 24.4, and 24.7 kcal/mol higher than IS1a, respectively. IS2a comes from IS1a via a three-membered ring transition state TS1 with an imaginary frequency of 383.3 cm^{-1}, and a barrier of 23.8 kcal/mol. During this transformation, the O_6—N_7 bond in IS1a is gradually broken and a new O_6—O_8 bond is gradually formed. In TS1, the O_6….O_8 distance is

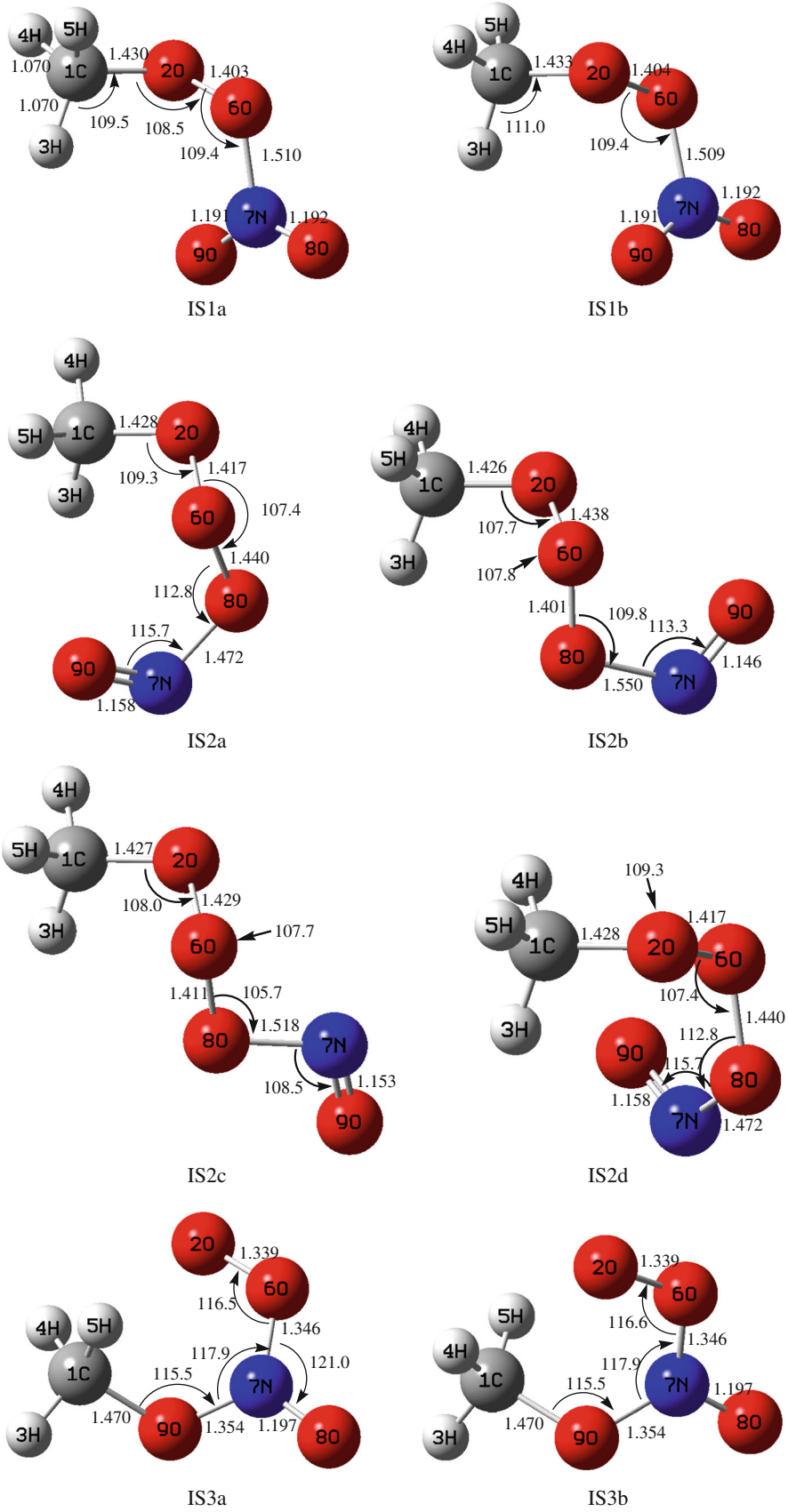

Fig. 1 Geometric parameters of related molecules on the $CH_3O_2NO_2$ energy surface at B3LYP/6-311G(2d,2p) level of theory. Bond lengths are in angstroms and bond angles are in degrees

Fig. 1 continued

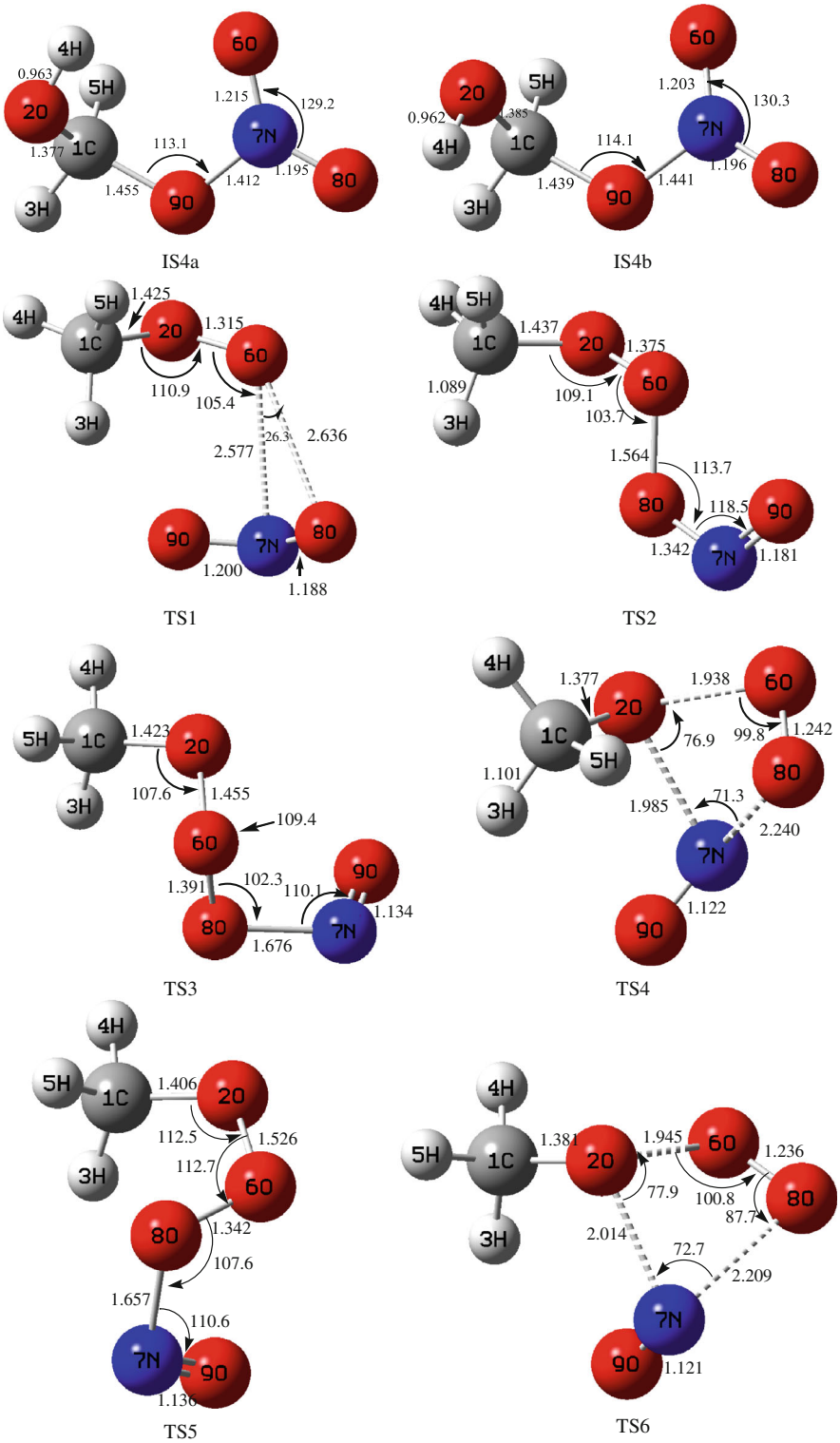

Fig. 1 continued

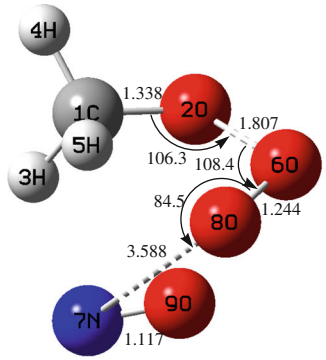

TS7

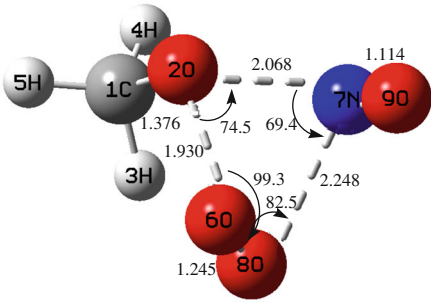

TS8

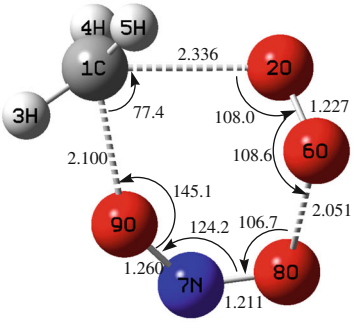

TS9

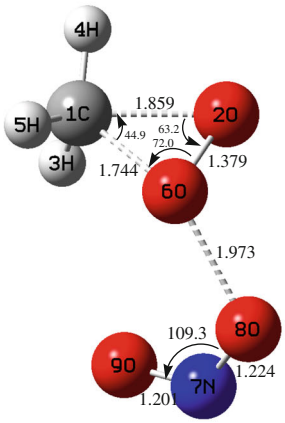

TS10

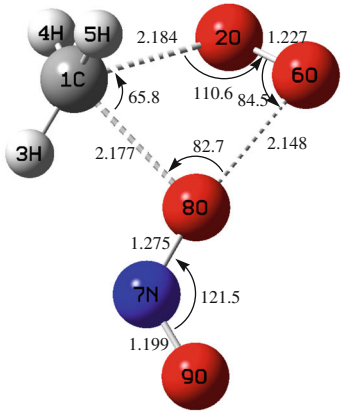

TS11

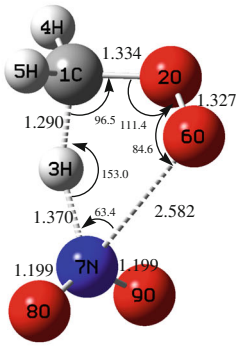

TS12

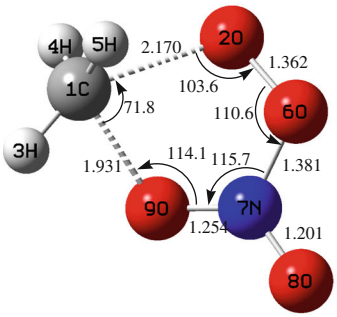

TS13

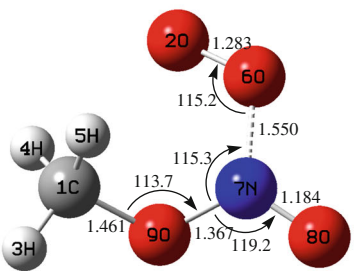

TS14

Fig. 1 continued

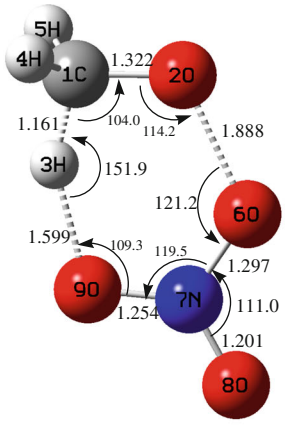

TS15

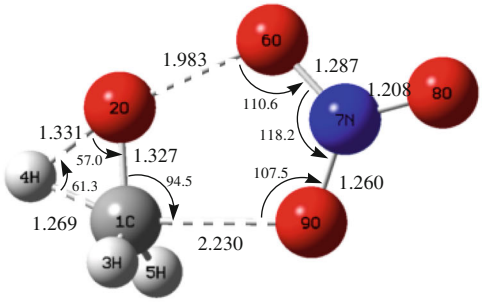

TS16

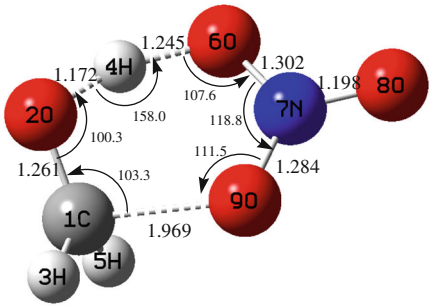

TS17

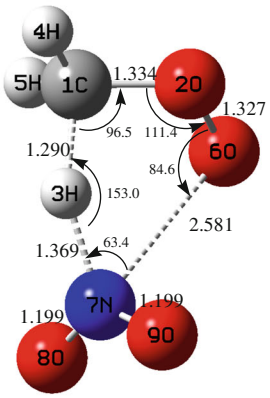

TS18

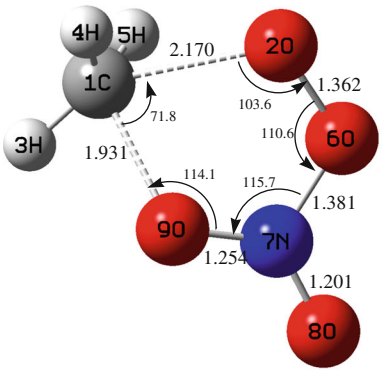

TS19

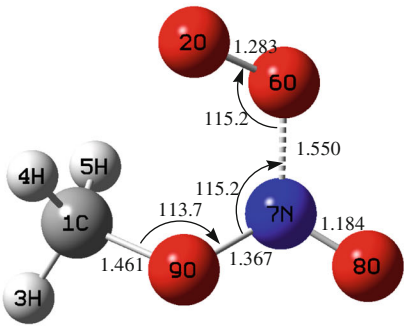

TS20

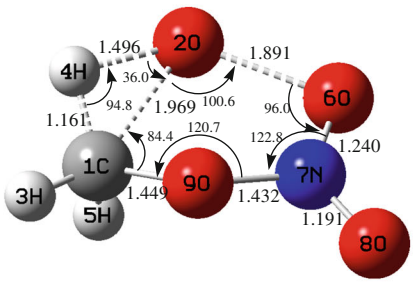

TS21

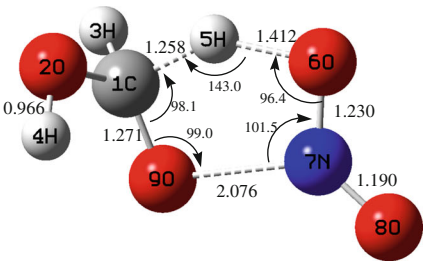

TS22

Fig. 1 continued

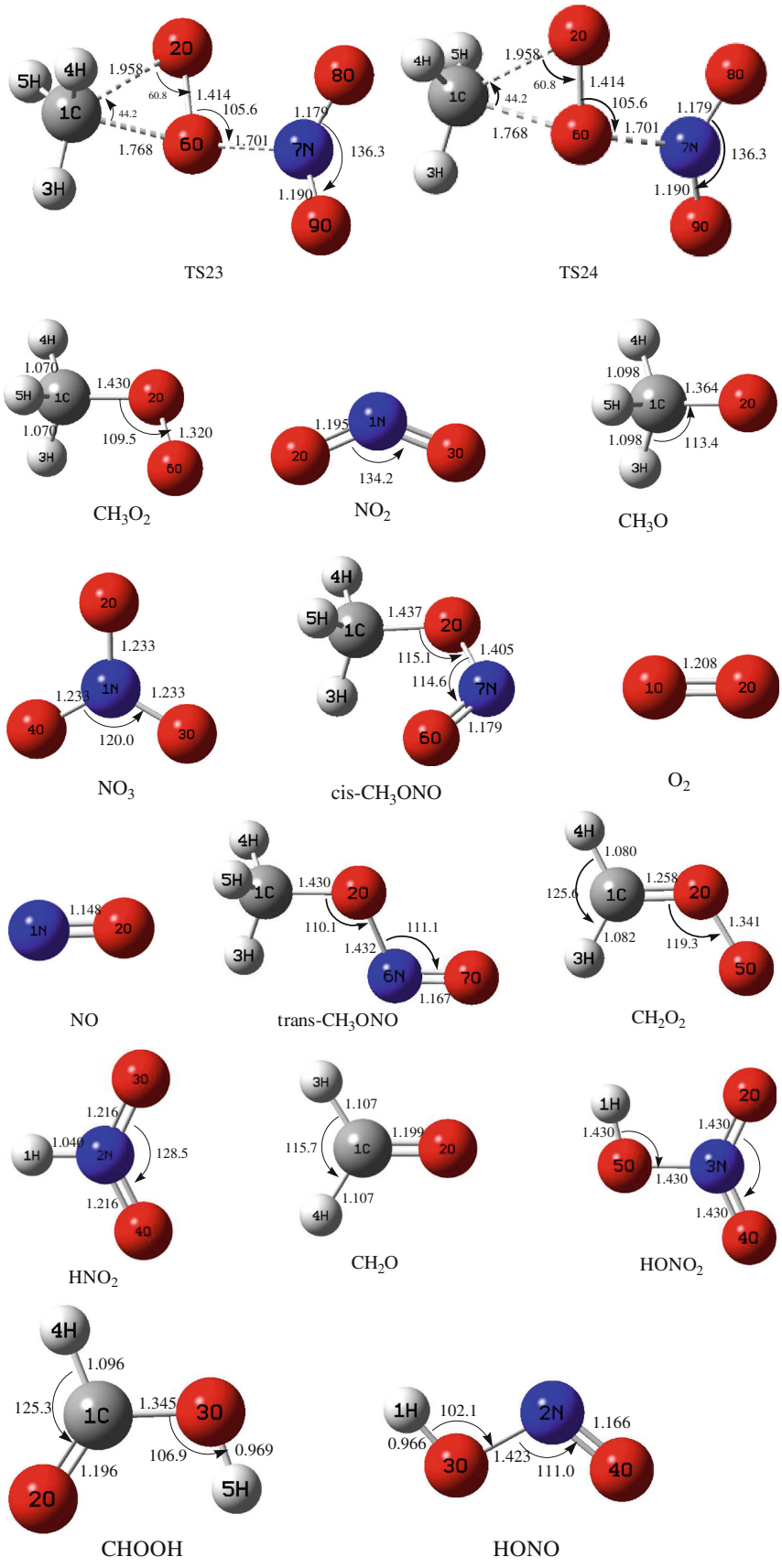

Table 1 Zero-point vibrational energies (ZPE, in kcal/mol), entropy S (in cal mol^{-1} K^{-1}), Gibbs free energies (ΔG, in kcal/mol) at 298.15 K, and relative energies (RE1, in kcal/mol) of the reactants, dissociation products and transition states calculated at the B3LYP/6-311G(2d, 2p) and CCSD(T)/cc-PVDZ levels

Species	B3LYP/6-311G(2d,2p)			CCSD(T)/cc-PVDZ	Other results				
	ZPE[a]	S	ΔG	RE1	RE2[b]	RE3[c]	RE4[d]	RE5[e]	RE6[f]
IS1a[g]	34.4	78.1	0.0	0.0	0.0	0.0	0.0	0.0	0.0
IS1b	34.4	78.1	0.0	0.0	0.0	0.0	2.0	2.0	2.0
IS2a	32.5	81.5	25.9	24.7	25.7	25.9	31.5	28. 9	28.2
IS2b	32.6	81. 4	24.0	22.5	23.5	23.7	26.2	26.1	25.4
IS2c	32.6	81.6	25.5	24.4	25.0	25.0	27.3	27.3	26.4
IS2d	32.5	81.5	25.9	24.7	25.7	25.9	31.5	28.9	28.2
IS3a	33.5	78.8	49.0	53.8	51.3	52.7	48.2	47.6	47.4
IS3b	33.5	78.9	49.0	53.8	51.3	52.7	48.2	47.6	47.4
IS4a	36.2	75.8	−54.9	−58.5	−60.4	−60.7		−55.8	−56.0
IS4b	35.9	77.2	−53.9	−56.8	−58.8	−59.1	−55.6		−56.0
$CH_3O_2 + NO_2$	31.0	121.9	5.7	20.8	20.9	21.0	23.3	23.0	22.0
$CH_3O + NO_3$	28.1	120.0	15.5	38.4	37.4	37.7	33.9	34.5	34.6
cis-$CH_3ONO + O_2$	31.3	116.0	−16.6	−10.1	−8.9	−9.1	−3.1	−4.1	−5.2
trans-$CH_3ONO + O_2$	31.1	117.3	−16.0	−7.9	−7.5	−7.7	−2.2	−3.4	−4.5
$CH_3O + NO + O_2$	26.7	154.7	10.0	29.6	31.3	30.7	38.8	37.5	35.6
$CH_2O_2 + HNO_2$	32.0	117.8	18.9	33.3	31.1	31.5	27.5	26.5	25. 4
$CH_2O + HONO_2$	33.0	117.1	−55.3	−43.7	−45.1	−45.4	−46.6	−46.8	−47.5
CHOOH + HONO	32.6	118.6	−103.3	−94.5	−97.5	−97.6	−96.2	−97.1	−98.7
TS1[h]	31.9	83.5	45.0	23.8	26.8	24.7	27.0	27.8	27.0
TS2	32.3	78.0	28.5	28.0	29.5	29.5	30.7	29.2	28.6
TS3	31.9	79.9	34.6	32.4	34.0	33.9	33.5	33.6	32.6
TS4	31.5	79.2	50.3	50.2	60.4	52.9	56.3	62.3	62.0
TS5	32.3	78.0	31.6	29.7	31.6	31.9	31.3	30.9	30.0
TS6	31.4	80.3	50.9	51.7	72.2	54.3	57.7	81.7	81.6
TS7	30.5	81.5	64.2	63.6	52.9	66.1	69.1	88.3	87.4
TS8	31.5	78.7	49.3	50.9	50.9	53.3	56.2		51.5
TS9	30.3	83.0	87.5	92.1	95.0	94.6	95.2	96.8	96.2
TS10	30.7	84.3	95.1	93.5	95.9	95.7	92.3	92.1	92.0
TS11	30.3	84.2	93.9	98.3	99.1	99.7	99.1	97.2	96.5
TS12	30.4	80.9	43.0	49.2	49.0	48.8	44.9	44.6	44.2
TS13	32.6	75.9	68.8	77.6	76.3	78.0	71.1	69.5	69.6
TS14	32.6	78.1	50.4	52.4	55.7	52.3	47.8	58.3	58.4
TS15	31.2	78.9	29.5	35.5	35.7	36.9	33.5	32.0	32.8
TS16	30.9	77.4	43.9	53.1	52.2	53.8	48. 1	46.5	46.3
TS17	32.5	75.2	−36.9	−33.5	−33.6	−33.6	−36.9	−37.6	−37.3
TS18	30.4	80.9	43.0	49.2	49.0	48.8	44.9	44.6	44.2
TS19	32.6	75.9	68.8	77.6	76.3	78.0	71.1	69.5	69.6
TS20	32.6	78.0	50.4	52.4	55.7	52.3	47.8	58.3	69.6
TS21	31.2	76.6	102.1	105. 2	105.9	106.4	103.0		
TS22	31.3	76.8	−21.1	−16.4	−17.6	−17.5	−21.1		−21.9
TS23	32.0	81.1	76.9	83.0	83.6	84.3	77.3	76.6	76.9
TS24	32.0	81.1	76.9	83.0	83.6	84.3	77.3	76.6	76.9

[a] Scaled by a factor of 0.96

[b] The values are obtained at QCISD(T)/6-311G(d, p) level

[c] The values are obtained at CCSD(T)/6-311G(d, p)

[d] The values are obtained at CBS-QB3 level

[e] The values are obtained at G3B3 level

[f] The values are obtained at G3MP2B3 level

[g] The total energy is −394.3855084 hartree

[h] IRC calculations of the reactions associated with these transition states are performed at the B3LYP/6-31G(d,p) levels

shortened to 2.636 Å, while the breaking O_6—N_7 bond is elongated from 1.510 Å in IS1a to 2.577 Å. Note that the energy of IS2a is abnormally 0.9 kcal/mol higher than TS1, which may be caused by the calculation accuracy. This pathway has been confirmed by IRC calculations and the reaction is endothermic by 24.7 kcal/mol. Then passing a

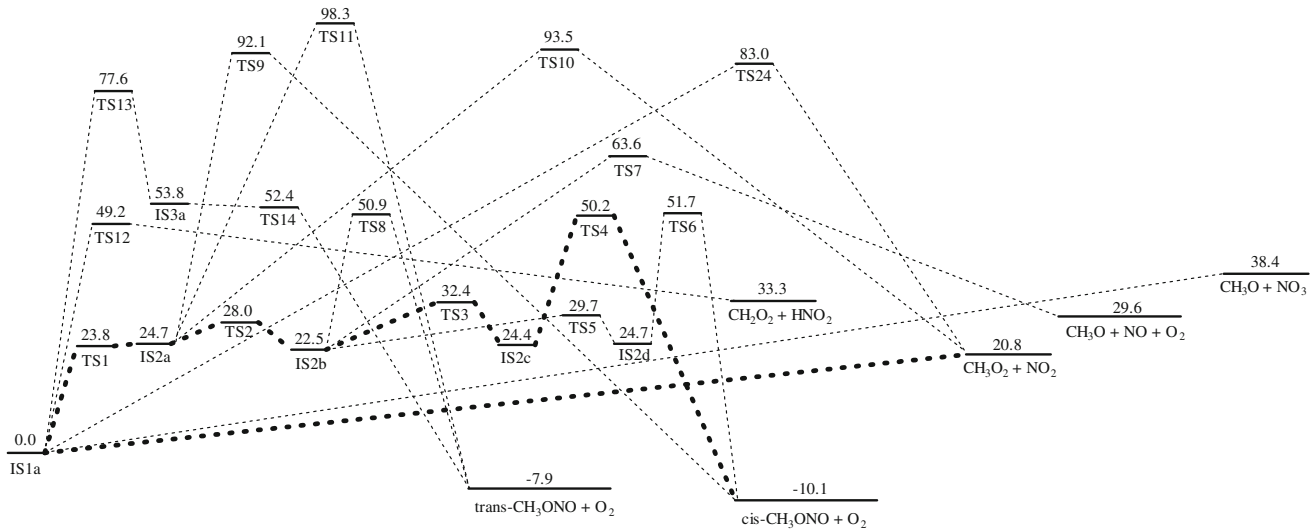

Fig. 2 CCSD(T)/cc-pVDZ//B3LYP/6-311G(2d,2p) potential energy diagram for the reaction pathways initiated from IS1a. The most feasible reaction channels are delineated in *bold lines*. The energies are in kcal/mol

transition state TS2 with a small imaginary frequency of 37.0 cm^{-1}, which corresponds to the internal rotation of the N_7—O_9 bond around the N_7—O_8 axis, IS2a isomerizes to IS2b over a low energy barrier of 3.3 kcal/mol. And IS2b can turn into IS2c via TS3 with a barrier height of 9.9 kcal/mol corresponding to the internal rotation of the O_9 atom around the N_7—O_9 axis. IS2b also can isomerize to IS2d via TS5 with a barrier of 7.2 kcal/mol. It initiates by the rotation of the $O_6O_8N_7O_9$ group around the O_2—O_6 axis.

IS3, $CH_3ON(O)O_2$

A pair of mirror image isomers has been found, named IS3a and IS3b. The structures of them are almost the same except the dihedral angles. For example, the dihedral angle among O_9, N_7, O_6, and O_2 atoms is −4.1° in IS3a, while it is 4.1° in IS3b. And the dihedral angle among O_8, N_7, O_6, and O_2 atoms is 169.1° in IS3a, while it is −169.1° in IS3b. Thus, this pair of mirror image isomers has the same energies from the calculated results.

The isomerization reaction, IS1a to IS3a via a five-membered ring transition state TS13, has a high barrier of 77.6 kcal/mol and an imaginary frequency of 552.0 cm^{-1}, endothermic by 53.8 kcal/mol. In this process, the C_1—O_2 bond in IS1a is gradually opened and the C_1—O_9 bond is gradually formed. The length of the C_1—O_2 bond is stretched to 2.170 Å in and the C_1….O_9 distance is shortened to 1.931 Å in TS13. The high energy barrier indicates that this process is hard to occur. Similarly, IS1b can isomerize to IS3b via TS19, which has the same energy and imaginary frequency as TS13.

IS4, $CH_2(OH)ONO_2$

IS4a and IS4b are conformational isomers and the energies of them are −58.5 and −56.8 kcal/mol, respectively. IS1b transforms to IS4a via TS16 with a barrier of 53.1 kcal/mol and an imaginary frequency of 1236.1 cm^{-1}. There are a five-membered and a three-membered rings in the structure of TS16. In this isomerization process, the C_1—H_4 and O_2—O_6 bonds in IS1b are gradually opened and the C_1—O_9 and O_2—H_4 bonds are gradually formed. In TS16, the length of the C_1—H_4 and O_2—O_6 bonds are elongated to 1.269 and 1.983 Å, respectively, while the C_1….O_9 and O_2…H_4 distances are shortened to 2.230 and 1.331 Å, respectively.

Over TS21, IS3b turns to IS4b with a barrier of 51.4 kcal/mol and an imaginary frequency of 1250.4 cm^{-1}. In this pathway, the C_1—H_4, and O_2—O_6 bonds are gradually elongated from 1.081 and 1.339 Å in IS3b to 1.161 and 1.891 Å in TS21, respectively. On the contrary, the C_1….O_2 and O_2….H_4 distances are shortened to 1.969 and 1.496 Å, respectively. This process is exothermic by 110.6 kcal/mol.

Unimolecular decomposition pathways of $CH_3O_2NO_2$

Pathway A: to produce $CH_3O_2 + NO_2$

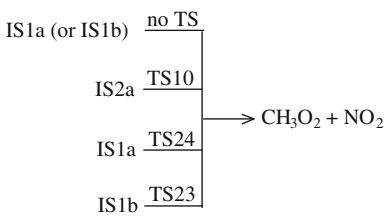

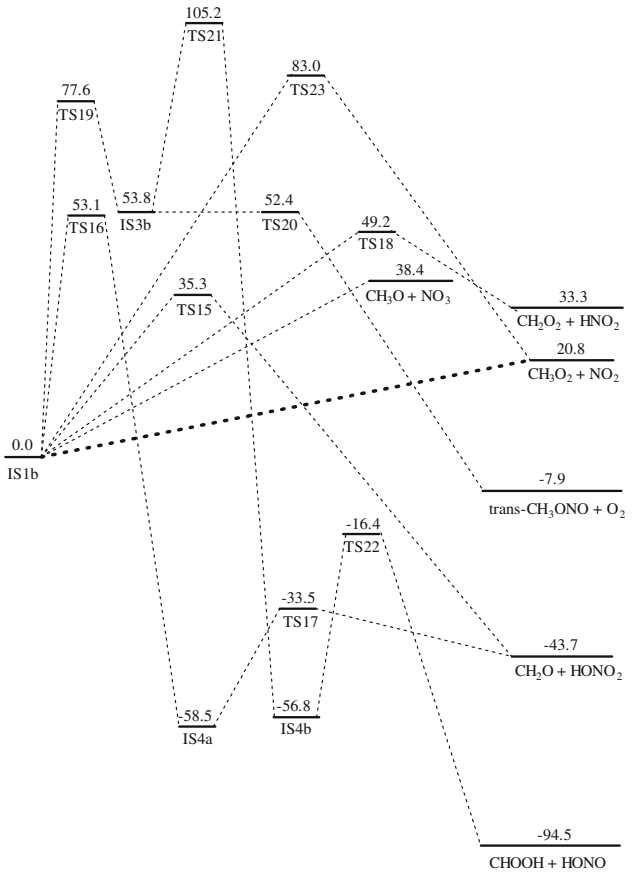

Fig. 3 CCSD(T)/cc-pVDZ//B3LYP/6-311G(2d,2p) potential energy diagram for the reaction pathways initiated from IS1b. The most feasible reaction channels are delineated in *bold lines*. The energies are in kcal/mol

There are four different paths to obtain the products CH_3O_2 and NO_2. The first one is the direct O_6—N_7 bond breaking in IS1a or IS1b with no transition state. The calculated O–N bond dissociation energy (BDE) is 20.8 kcal/mol at CCSD(T)/cc-PVDZ level, agreeing very well with the experimental active energy given by Zabel et al., which is 20.7 kcal/mol [7]. From Table 1, we can know that the energy has also been confirmed by QCISD(T)/6-311G(d,p), CCSD(T)/6-311G(d, p), CBS-QB3, G3B3, and G3MP2B3 methods, and it is 20.9, 21.0, 23.3, 23.0, and 22.0 kcal/mol, respectively. Obviously, these values calculated at different levels agree very well.

The second path is via TS10 with a barrier of 68.8 kcal/mol, IS2a dissociates to the above products. During this process, the C_1—O2 and O_6—O8 bonds in IS2a are slowly opened and a new C_1—O_6 bond is formed. TS10 has a COO three-membered ring in its structure and the length of the C_1—O2 and O_6—O8 bonds are stretched to 1.895 and 1.973 Å, respectively, while the C_1….O_6 distance is shortened to 1.744 Å. This path is exothermic by 4.1 kcal/mol, which is difficult to occur because of the high energy barrier.

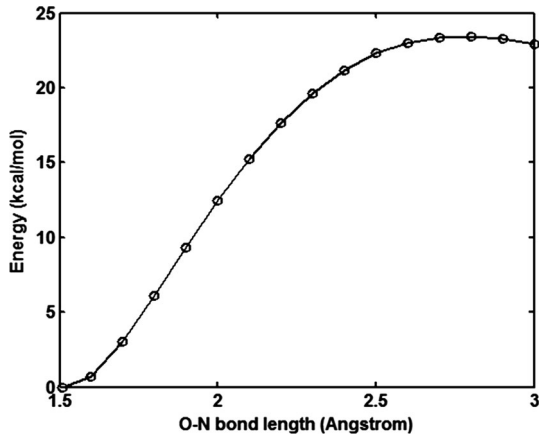

Fig. 4 Scanning of the potential energy surface along the O–N bond in IS1a. The energies are calculated at CCSD(T)/cc-pVDZ level

The third channel is IS1a decomposes to CH_3O_2 and NO_2 via a three-membered ring transition state TS24 with an imaginary frequency of 899.8 cm^{-1} and a high barrier of 83.0 kcal/mol. In this process, the C_1—O_2 and O_6—N_7 bonds in IS1a are gradually opened and a new C_1—O_6 bond is slowly formed. In the structure of TS24, the length of the C_1—O_2 and O_6—N_7 bonds are elongated to 1.958 and 1.701 Å, respectively, yet the forming of the C_1….O_6 distance is shortened to 1.768 Å. This process is endothermic by 20.8 kcal/mol.

The last path is IS1b dissociates to the designated products via a three-membered ring transition state TS23. From Fig. 1, we can see that the bond lengths and bond angles of TS23 are the same to those in TS24. The main differences between the structures of these two transition states are the dihedral angles. For example, the dihedral angle among N_7, O_6, O_2, and C_1 atoms is 140.3° in TS24, while it is −140.3° in TS23. Thus, this reaction process is similar to the third channel, and we shall not discuss it again.

Now the question is there are two paths to produce CH_3O_2 plus NO_2 from IS1a and IS1b, respectively. One is the direct O_6—N_7 bond rupture via no transition state with the 20.7 kcal/mol BDE, the other is the concerted bond cleavage via a three-membered ring transition state with a high barrier of 83.0 kcal/mol where there are two bonds breaking and a new bond forming. To make sure there is indeed no obvious transition state for the direct O_6—N_7 bond rupture, we have scanned the PESs along the O_6—N_7 bond in IS1a at CCSD(T)/cc-pVDZ level. The results are shown in Fig. 4. When the O_6—N_7 bond is stretched to about 2.8 Å, the energy of IS1a reaches maximum value of 23.5 kcal/mol, which is similar to a transition state. This energy is a little larger than the O–N BDE (20.8 kcal/mol) and the experimental active energy (20.7 kcal/mol) [7]. Therefore IS1a and IS1b prefer to dissociate into CH_3O_2

and NO_2 by direct O_6—N_7 bond cleavage because of the lower energy barriers.

Pathway B: to produce $CH_3O + NO_3$

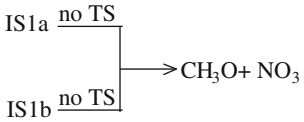

We have not found the transition state for the O_2—O_6 bond cleavage in IS1a or IS1b to yield CH_3O and NO_3. The calculated O–O BDE is 38.4 kcal/mol at CCSD(T)/cc-PVDZ level, confirmed by QCISD(T)/6-311G(d, p), CCSD(T)/6-311G(d, p), CBS-QB3, G3B3, G3MP2B3 methods, which is 37.4, 37.7, 33.9, 34.5, and 34.6 kcal/mol, respectively. From the calculated results, we can know that the O–O BDE is 17.6 kcal/mol higher than the O–N BDE, thus this path is more difficult to occur.

Pathway C: to produce cis-$CH_3ONO + O_2$

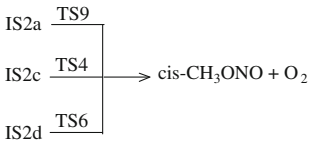

Three pathways have been found to produce *cis*-CH_3ONO and O_2. The first one is IS2a dissociation via a six-membered ring transition state TS9 with a high barrier of 67.4 kcal/mol and an imaginary frequency of 497.6 cm^{-1}. In this process, the C_1—O_2 and O_6—O_8 bonds in IS2a are gradually opened and the C_1—O_9 bond is gradually formed. In TS9, the length of the C_1—O_2 and O_6—O_8 bonds are elongated to 2.336 and 2.051 Å, respectively, while the C_1….O_9 distance is shortened to 2.100 Å. This process is exothermic by 34.8 kcal/mol. The second path is IS2c decomposition via a four-membered ring transition state TS4 with an imaginary frequency of 210.6 cm^{-1} and a low barrier of 25.8 kcal/mol. This process undergoes the O_2—O_6 and N_7—O_8 bonds in IS2c breaking and the O_2—N_7 bond forming. The opening O_2—O_6 and N_7—O_8 bonds in TS4 are stretched by 0.509 and 0.722 Å, respectively, while the O_2…. N_7 distance is shortened to 1.985 Å. This process is exothermic by 34.5 kcal/mol. And the third path is IS2d dissociation via a four-membered ring transition state TS6 with a barrier of 27.0 kcal/mol. TS6 has an imaginary frequency of 245.2 cm^{-1} and in its structure, the breaking O_2—O_6 and N_7—O_8 bonds are lengthened to 1.945 and 2.209 Å, respectively, while the forming O_2…. N_7 distance is shortened to 2.014 Å. This process is also exothermic by 34.8 kcal/mol.

Pathway D: to produce trans-$CH_3ONO + O_2$

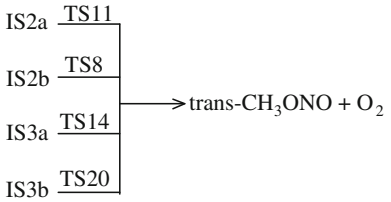

We have found four paths to obtain the products *trans*-CH_3ONO and O_2. First of all, IS2a decomposition through a four-membered ring transition state TS11 with a high barrier of 73.6 kcal/mol suggests that this reaction is hard to occur. During the process, the C_1—O_2 and O_6—O_8 bonds in IS2a are gradually elongated and the C_1….O_8 distance is gradually shortened to form a four-membered ring. The imaginary frequency of TS11 is 569.6 cm^{-1} and in TS11 the length of the C_1—O_2 and O_6—O_8 bonds are elongated to 2.184 and 2.148 Å, respectively, while the forming C_1….O_8 distance is shortened to 2.177 Å. This process is exothermic by 32.6 kcal/mol.

The second one is IS2b dissociation via a four-membered ring transition state TS8 with a small barrier of 28.4 kcal/mol and an imaginary frequency of 221.9 cm^{-1}. In this process, the O_2—O_6 and N_7—O_8 bonds in IS2b are gradually elongated and the O_2….N_7 distance is gradually shortened to form a four-membered ring. In the structure of TS8, the breaking O_2—O_6 and N_7—O_8 bonds are elongated to 1.930 and 2.248 Å, respectively, while the forming O_2….N_7 distance is shortened to 2.068 Å. This process is exothermic by 30.4 kcal/mol.

The third and fourth paths are IS3a and IS3b decomposition via TS14 and TS20, respectively. These two paths have the similar process, both undergoing the direct O_6—N_7 bonds rupture. The structures of TS14 and TS20 are like a pair of mirror image isomers, which have the same imaginary frequencies, bond lengths and bond angles, unless the dihedral angles. The breaking O_6—N_7 bonds in these two transition states are both stretched to 1.550 Å. The energies of TS14 or TS20 are abnormally 1.4 kcal/mol lower than IS3a or IS3b, which may be caused by the calculation accuracy. These two paths are both exothermic by 61.7 kcal/mol.

Pathway E: to produce $CH_3O + NO + O_2$

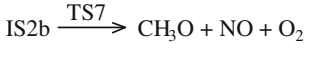

Only one path has been found to produce the products CH_3O plus NO and O_2. This process is IS2b decomposition

via TS7 with an imaginary frequency of 208.3 cm^{-1} and an energy barrier of 41.1 kcal/mol. In TS7, the breaking O_2—O_6 and N_7—O_8 bonds are elongated to 1.807 and 3.588 Å, respectively. This direct bonds rupture is endothermic by 7.1 kcal/mol.

Pathway F: to produce $CH_2O_2 + HNO_2$

$$\begin{matrix} \text{IS1a} \xrightarrow{\text{TS12}} \\ \qquad\qquad\quad \longrightarrow CH_2O_2 + HNO_2 \\ \text{IS1b} \xrightarrow{\text{TS18}} \end{matrix}$$

IS1a and IS1b dissociate to the products $CH_2O_2 + HNO_2$ via five-membered rings transition states TS12 and TS18, respectively, with the same energy barrier of 49.2 kcal/mol. These two transition states are like a pair of mirror image isomers, which almost have the same bond lengths and bond angles, unless the dihedral angles. The imaginary frequency of TS12 is 1050.4 cm^{-1}, and in its structure the length of the C_1—H_3 and O_6—N_7 bonds are stretched to 1.290 and 2.582 Å, respectively, while the forming H_3….N_7 distance is shortened to 1.370 Å. Similarly, the imaginary frequency of TS18 is 1051.0 cm^{-1}, and the length of the C_1—H_3 and O_6—N_7 bonds are stretched to 1.290 and 2.581 Å, respectively, while the forming H_3….N_7 distance is shortened to 1.369 Å. These two paths are both endothermic by 33.3 kcal/mol.

Pathway G: to produce $CH_2O + HONO_2$

$$\begin{matrix} \text{IS1b} \xrightarrow{\text{TS15}} \\ \qquad\qquad\quad \longrightarrow CH_2O + HONO_2 \\ \text{IS4a} \xrightarrow{\text{TS17}} \end{matrix}$$

There are two paths to produce CH_2O and $HONO_2$. One is IS1b dissociation via a six-membered ring transition state TS15 with a barrier of 35.3 kcal/mol, and the other is IS4a decomposition via TS17 with an imaginary frequency of 992.7 cm^{-1} and a barrier of 25.0 kcal/mol. The imaginary frequency of TS15 is 693.8 cm^{-1} and in TS15 the length of the C_1—H_3 and O_2—O_6 bonds are elongated to 1.161 and 1.888 Å, respectively, yet the forming H_3….O_9 distance is shortened to 1.599 Å. This process is exothermic by 43.7 kcal/mol. TS17 also has a six-membered ring in its structure, and the breaking O_2—H_4 and C_1—O_9 bonds are elongated to 1.172 and 1.969 Å, respectively, while the forming H_4….O_6 distance is shortened to 1.245 Å. This path is endothermic by 14.8 kcal/mol.

Pathway H: to produce CHOOH + HONO

$$\text{IS4b} \xrightarrow{\text{TS22}} \text{CHOOH} + \text{HONO}$$

Via a five-membered ring transition state TS22 with a barrier of 40.4 kcal/mol and an imaginary frequency of 1212.6 cm^{-1}, IS4b dissociates to the products CHOOH plus HONO. In this process, the C_1—H_5 and N_7—O_9 bonds in IS4b are gradually opened and the H_5….O_6 distance is gradually shortened. In the structure of TS22, the length of the C_1—H_5 and N_7—O_9 bonds are elongated to 1.258 and 2.079 Å, respectively, while the forming H_5….O_6 distance is shortened to 1.412 Å. This process is exothermic by 37.7 kcal/mol.

Feasible reaction paths

The results discussed above show that the most feasible decomposition pathways for $CH_3O_2NO_2$ are those leading to $CH_3O_2 + NO_2$ and *cis*-$CH_3ONO + O_2$, and the former is the lowest-energy path (See Figs. 2, 3). Their energy barriers are listed in parentheses.

$$\text{IS1a (or IS1b)} \xrightarrow{\text{no TS}} CH_3O_2 + NO_2 \quad (20.8\ \text{kcal/mol})$$

$$\text{IS1a} \longrightarrow \text{TS1IS2a} \xrightarrow{\text{TS2}} \text{IS2b} \xrightarrow{\text{TS3}} \text{IS2c} \xrightarrow{\text{TS4}} \textit{cis}\text{-}CH_3ONO + O_2 \quad (25.8\text{kcal/mol, imposed by TS4}).$$

Furthermore, the barrier of IS1a isomerization to IS2a is 23.8 kcal/mol, close to the 20.8 kcal/mol O–N BDE in IS1a or IS1b, thus the isomerization reaction may compete with the direct bond rupture dissociation reaction.

Based on the calculated CCSD(T)/cc-pVDZ PES, we have probed qualitatively the possible unimolecular decomposition and isomerization reaction mechanism of methyl peroxynitrate. Our discussion does not take the entropy factor into account, which also plays an important role in determining the kinetics and thermodynamics of a reaction. The entropies and Gibbs free energies of the relevant isomers, transition states and products obtained at B3LYP/6-311G(2d,2p) level are also listed in Table 1. In general, the Gibbs free energies are consistent with the energies obtained by high level methods except TS1. The energy of TS1 is 23.8 kcal/mol at CCSD(T)/cc-pVDZ level, in good agreement with the values obtained by other methods, while the Gibbs free energy is 45.0 kcal/mol at B3LYP/6-311G(2d,2p) level. Then we check the electronic energy obtained at B3LYP/6-311G(2d,2p) level, and find that it is 48.7 kcal/mol, 24.9 kcal/mol higher than the energy obtained at CCSD(T)/cc-pVDZ level. Therefore DFT overestimates the electronic energy of TS1.

The values of the entropies of the isomers and transition states are closely around 80.0 cal mol^{-1} k^{-1}. Certainly, those fragmentation products have the highest entropies and will be considerably stabilized with respect to $CH_3O_2NO_2$ on the Gibbs energy profile. Thus, when we take entropy into consideration, the energy profile is not expected to change significantly, and our conclusions will generally not be affected.

Conclusions

The complex PESs for the unimolecular isomerization and decomposition of methyl peroxynitrate ($CH_3O_2NO_2$), including 10 isomers, 24 interconversion transition states and 15 major dissociation products, are probed theoretically at the CCSD(T)/cc-pVDZ//B3LYP/6-311G(2d,2p) level of theory. The geometries and relative energies for various stationary points are determined. The results show that there are the two most stable isomers, IS1a and IS1b, which are a pair of mirror image isomers. From IS1a and IS1b, different isomerization and unimolecular decomposition reaction channels have been studied and discussed. Among them, the predominant thermal decomposition pathways are those leading to $CH_3O_2 + NO_2$ from IS1a (or IS1b) and *cis*-$CH_3ONO + O_2$ from IS2c, while the former is the lowest-energy path. The potential surface along the O–N bond in IS1a has been scanned at CCSD(T)/cc-pVDZ level, where the energy of IS1a reaches maximum value of 23.5 kcal/mol when the O–N bond is stretched to about 2.8 Å. This energy is a little larger than the O–N BDE (20.8 kcal/mol) and the experimental active energy (20.7 kcal/mol). Furthermore, the energy barriers of IS1a isomerization to IS2a are 23.8 kcal/mol, close to the 20.8 kcal/mol O–N BDE in IS1a or IS1b, thus the isomerization reaction may compete with the direct bond rupture dissociation reaction.

Acknowledgments This work is supported by the National Natural Science Foundation (NNSF) of China (20903101, 21103003).

References

1. Solomon S, Qin D, Manning M, Alley R, Berntsen T, Bindoff N, Chen Z, Chidthaisong A, Gregory J, Hegerl G, Heimann M, Hewitson B, Hoskins B, Joos F, Jouzel J, Kattsov V, Lohmann U, Matsuno T, Molina M, Nicholls N, Overpeck J, Raga G, Ramaswamy V, Ren J, Rusticucci M, Somerville R, Stocker T, Whetton P, Wood R A, Wratt D: Technical Summary. In: Climate Change 2007: The Physical Science Basis. Contribution of Working Group I to the Fourth Assessment Report of the Intergovernmental Panel on Climate Change, IPCC AR4, p74, 2007
2. Kley D (1997) Science 276:1043–1045
3. Wang YH, Jacob DJ, Logan JA (1998) J Geophys Res Atmos 103:10713–10725
4. Murphy JG, Thornton JA, Wooldridge PJ, Day DA, Rosen RS, Cantrell C, Shetter RE, Lefer B, Cohen RC (2004) Atmos Chem Phys 4:377–384
5. Sander SP, Watson RT (1980) J Phys Chem 84:1664–1674
6. Ravishankara AR, Eisele FL, Wine PH (1980) J Chem Phys 73:3743–3749
7. Zabel F, Reimer A, Becker KH, Fink EH (1989) J Phys Chem 93:5500–5507
8. Bridier I, Lesclaux R, Veyret B (1992) Chem Phys Lett 191:259–263
9. Golden DM (2005) Int J Chem Kinet 37:625–632
10. Becke AD (1993) J Chem Phys 98:5648–5652
11. Lee CT, Yang WT, Parr RG (1988) Phys Rev B 37:785–789
12. Foresman JB, Frisch A Exploring Chemistry with Electronic Structure Methods, second edition, Gaussian, Inc, Pittsburgh, PA, p64, 1995
13. Gonzalez C, Schlegel HB (1989) J Chem Phys 90:2154–2161
14. Bartlett RJ, Purvis GD (1978) Int J Quantum Chem 14:561–581
15. Woon DE, Dunning TH (1993) J Chem Phys 98:1358–1371
16. Pople JA, Head-Gordon M, Raghavachari K (1987) J Chem Phys 87:5968–5975
17. Montgomery JA, Frisch MJ, Ochterski JW, Petersson GA (1999) J Chem Phys 110:2822–2827
18. Montgomery JA, Frisch MJ, Ochterski JW, Petersson GA (2000) J Chem Phys 112:6532–6542
19. Curtiss LA, Raghavachari K, Redfern PC, Rassolov V, Pople JA (1998) J Chem Phys 109:7764–7776
20. Baboul AG, Curtiss LA, Redfern PC, Raghavachari K (1999) J Chem Phys 110:7650–7657
21. Frisch MJ, Trucks GW, Schlegel HB, Scuseria GE, Robb MA, Cheeseman JR, Montgomery JA, Jr., Vreven T, Kudin KN, Burant JC, Millam JM, Iyengar SS, Tomasi J, Barone V, Mennucci B, Cossi M, Scalmani G, Rega N, Petersson GA, Nakatsuji H, Hada M, Ehara M, Toyota K, Fukuda R, Hasegawa J, Ishida M, Nakajima T, Honda Y, Kitao O, Nakai H, Klene M, Li X, Knox JE, Hratchian HP, Cross JB, Bakken V, Adamo C, Jaramillo J, Gomperts R, Stratmann RE, Yazyev O, Austin AJ, Cammi R, Pomelli C, Ochterski JW, Ayala PY, Morokuma K, Voth GA, Salvador P, Dannenberg JJ, Zakrzewski VG, Dapprich S, Daniels AD, Strain MC, Farkas O, Malick DK, Rabuck AD, Raghavachari K, Foresman JB, Ortiz JV, Cui Q, Baboul AG, Clifford S, Cioslowski J, Stefanov BB, Liu G, Liashenko A, Piskorz P, Komaromi I, Martin RL, Fox DJ, Keith T, Al-Laham MA, Peng CY, Nanayakkara A, Challacombe M, Gill PMW, Johnson B, Chen W, Wong MW, Gonzalez C, Pople JA, Gaussian 03, revision E.01; Gaussian, Inc.: Wallingford CT, 2007